# Force and Deformation Behaviour of Roof Truss System with Cold-Formed Steel Channel Section

Tam Ping Hau [1,a], Mohd Syahrul Hisyam Mohd Sani [1,2,b], Cher Siang Tan[1,3,c*]
Yeong Huei Lee[1,d] Arizu Sulaiman[1,3,e] Shek Poi Ngian[4,f]

[1]Faculty of Civil Engineering, Universiti Teknologi Malaysia, Johor, Malaysia
[2]Faculty of Civil Engineering, Universiti Teknologi MARA, Pahang, Malaysia.
[3]Forensic Engineering Centre, Universiti Teknologi Malaysia, Johor, Malaysia
[4]Construction Research Centre, Universiti Teknologi Malaysia, Johor, Malaysia

[a] tphau2@live.utm.my, [b]msyahrul210@pahang.uitm.edu.my [c]tcsiang@utm.my, [d]yhlee7@live.utm.my, [e]arizu@utm.my, [f]shekpoingian@utm.my

**Keywords:** Cold-formed steel; roof truss; channel section; deformation

**Abstract.** Cold-formed steel is widely used in Malaysia's construction for roof truss structures. This study aims to investigate the force and deformation behaviour of a roof truss system and evaluate the results from analytical and experimental investigation. One roof truss was constructed by using LC7510 cold-formed steel channel which is 5.4m long and 0.651m height with angle about 20 degree and eight concentrated loads were acting on the top chord. The deflection of the roof truss was analyzed by LVDT's. STAAD Pro was used to carry out the analytical investigation. Three models with three load cases been modeled and compared with actual roof truss. The critical load case is Load Case 2 which leaded to higher deflections. The percentage difference on deflection between Model 1 with Load Case 2 is 15.4% and the roof truss failed on connection direct to the support due to buckling.

## Introduction

Cold-formed steel is widely used in Malaysia's construction for roof truss structures. By applying cold-formed steel (CFS) in the construction industry, it can contribute in terms of consuming less assembling time and is also promotes sustainability as compared to timber construction. Besides, replacing traditional wood roof system by cold-formed steel roof system may avoid insect and fungal infections as it will cause failure of the roof structure after long period of time. With the rapid emerged of the CFS in commercial and residential construction, a study should carry out to determine the behaviour of the CFS truss in order to achieve sustainability construction as there are a lot of over-design structures in the market. To achieve various changes of architectural design structures and to develop a better structural design, an innovation study about different truss arrangements may provide a suitable design for every structure using purpose.

A truss only experiences axial forces when load applied on it. The axial forces are tension force and compression force. For Howe truss, the vertical webs will experience compression forces while diagonal webs will under tension force [1]. The force of each roof truss members can be determined by the method of joints [2]. The entire truss is assumed in equilibrium then each of its joints is in equilibrium too. The force equilibrium equations obtain the member forces acting on each joint. Roof truss is considered as plane truss and subjected to two-force members lying in a single plane. To satisfy the equilibrium of each joint, the equilibrium force systems are $\Sigma F_x = 0$ and $\Sigma F_y = 0$. Then the force behaviour of the each roof truss member can be determined through the assumption positive and negative sign for tension and compression forces during calculation. To get the nodal displacement of the truss, it can be determine by the Stiffness Method. According to Hibbeler [3], the global force components $Q$ acting on the truss is related to its global displacements $D$ once the structure stiffness matrix $K$ is formed. The equation will be as below:

$$Q = KD \qquad \text{Eq. (1)}$$

$$D = K^{-1} Q \qquad \text{Eq. (2)}$$

From equation 2, the global displacement *D* can be determined by the invert stiffness matrix *K* multiply with global force components *Q*.

In stress-strain characteristic of steel, yield point and tensile strength determine the strength of the steel. Yield point of the cold-formed steel is crucial in characterizing its strength member and beyond that point, the elongation of the member elastically under load. Generally, there are two types of stress-strain curves which are sharp-yielding type and gradual-yielding type. These two types of curves are based on the manufacturing process of the steel. From Yu & LaBoube [4], the hot-rolling steel will experience sharp-yielding in stress-strain curve. While the yields stress behavior of cold-rolling steel is shown in gradual-yielding type. Hancock et al. [5] stated that high in yield strength may lead to reduction in ductility. Besides, the strength of the member also related to tensile strength. Tensile strength is the maximum tensile stress can be taken by a tension member before it breaks or undergoes permanent deformation. It specifies the point where a member undergoes elastic to plastic deformation. From a study done by Abdel-Rahman and Sivakumaran [6], the yield strength of flat and corner zones of lipped channel are different. The yield strength of the corner zone is higher than the flat zone.

As cold-formed steel is thin material and used in long span, there are several buckling modes will be undergo by cold-formed steel under compression. This is due to its slenderness that related width to thickness ratio. For C-channel section, the types of buckling are local buckling, torsional buckling and flexural torsional buckling [7]. From most of the previous research on C-channel roof truss, local buckling is the common buckling mode happened in compression members. Based on the research by Dawe et al. [8], the failure of C-channel roof truss initiated by the local buckling at one side of the top chord adjacent to the heel plate and followed by the buckling or crushing of the bottom chord at the same side as the buckled top chord. The research by Wood and Dawe [9] showed that the local buckling happened at the top chord adjacent to the heel plate due to compression as the materials were C-channel. Then a large deflection of a joint occurred near the location of local buckling happened.

Structural software is using for designing and analyzing the roof truss system nowadays. There are differences between actual constructing and analysis results due to different assumptions use in the software system as compared to the actual experiment. With different assumptions, this may lead to failure of roof truss in daily usage. In addition, CFS is a new material that used in Malaysia's construction industry and the industry is lack of experience in designing and applying it as the understanding about the behaviour of the CFS is still in preliminary stage. The differences between actual constructing and analysis results may lead to difficulties in designing the roof truss and cause the failure of roof truss system. The objectives of the research are to investigate the force and deformation behaviour of a roof truss system using analytical approach, to perform physical tests on the roof truss system, and to compare and evaluate the results from analytical and experimental investigation

**Methodology**

One type of roof truss had been constructed for this experiment which was Warren roof truss. The specimen was 5.4m long and 0.651m height. It was constructed in 20 degree slope of the top chord connected to bottom chord which AutoCAD drawing was presented in Figure 1. The channel section with lips was named as LC7510 that used as the experiment material for constructing the roof trusses in the experiment. It is channel with lips which shows in Figure 2. From Table 1, the dimensions of LC7510 are stated.

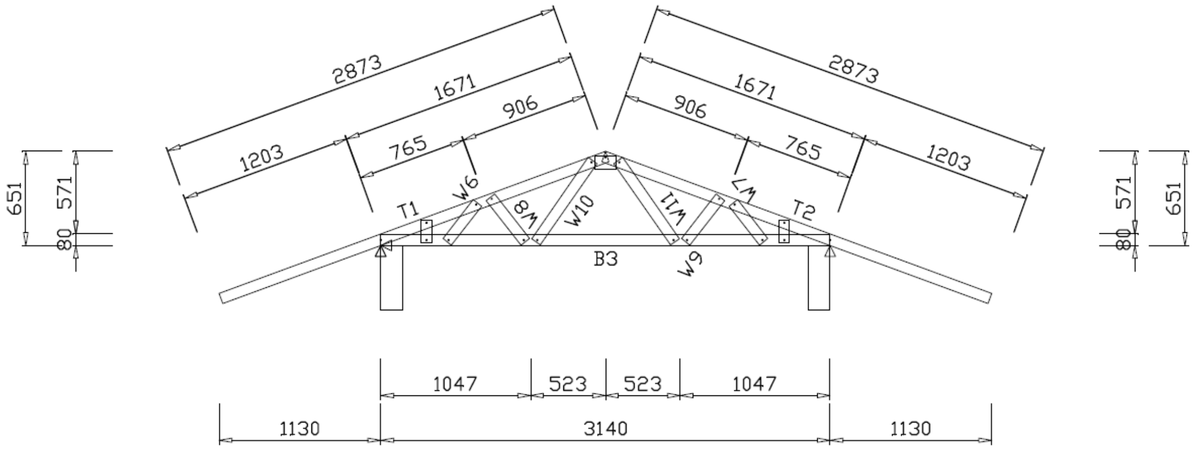


Figure 1: Dimensions of 5.4m Warren roof truss

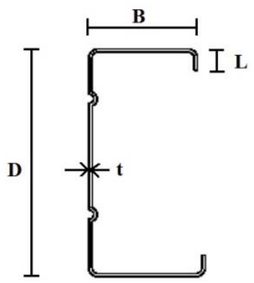


Figure 2: Cross sectional profile of cold-formed steel lipped channel section LC7510

Table 1: Section properties of LC7510

| **Material Name** | LC 7510 | |
|---|---|---|
| Section Dimension | Web, D (mm) | 75.0 |
| | Flange, F (mm) | 37.0 |
| | Lipped, L (mm) | 8.0 |
| | Thickness, t (mm) | 1.0 |
| **Area** | $A$(mm$^2$) | 162.99 |
| **Second Moment of Area** | $I_{xx}$ (mm$^4$) | 154249 |
| | $I_{yy}$ (mm$^4$) | 29220 |
| **Second Modulus** | $Z_{xx}$ (mm$^3$) | 4052 |
| | $Z_{yy}$ (mm$^3$) | 1116 |
| **Radius of Gyration** | $r_x$ (mm) | 30.76 |
| | $r_y$ (mm) | 13.39 |
| **Weight** | Wt (kg/m) | 1.282 |
| **Yield Strength** | $f_y$ (MPa) | 550 |
| **Torsion Constant** | J (mm$^4$) | 76.38 |

In this laboratory testing, four self-drilling screws were used for every connection on the roof truss (Figure 3(a) and (b)). The self-drilling screws were about 5 mm for diameter.

(a) Connection at LVDT 7 and support

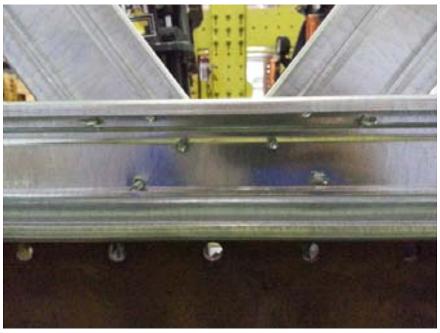

(b) Connection of intermediate members on the right hand-side to the bottom chord

Figure 3: Connections

According to Figure 4 below, it shows the drawing of setting up for roof truss testing. The Magnus frame was set up by hot-rolled I-beam with bolts and nuts to carry the roof truss experimental testing. The load applied was through eight solid wooden blocks with 20 degree. Each solid wooden block was screwed with a steel plate that can hold the steel treaded rod with a nut. Then the wooden blocks were screwed directly on the top chord of the roof truss acted as the load acting point. The eight solid wooden blocks spaced about 330mm horizontally from each other on the top chord of the roof truss. The steel treaded rods were hold from the steel plates with nuts from top chord to hang a spreader beam below from the roof truss. Then the applied load from hydraulic jack acted on the top chord of roof truss uniformly as point loads by eight solid wooden blocks through the spreader beam connected to the steel treaded rods. Seven LVDTs were set under the bottom chord of the roof truss. LVDT 4 was set at the mid-span of the bottom chord while others were located at each node of the intermediate members connected to the bottom chord. Then, the deflection at the nodes on bottom chord and mid-span were determined. The roof trusses were braced in Z-axis by hot-rolled angle steel members with wooden blocks to allow the roof trusses deflected in X and Y-axis.

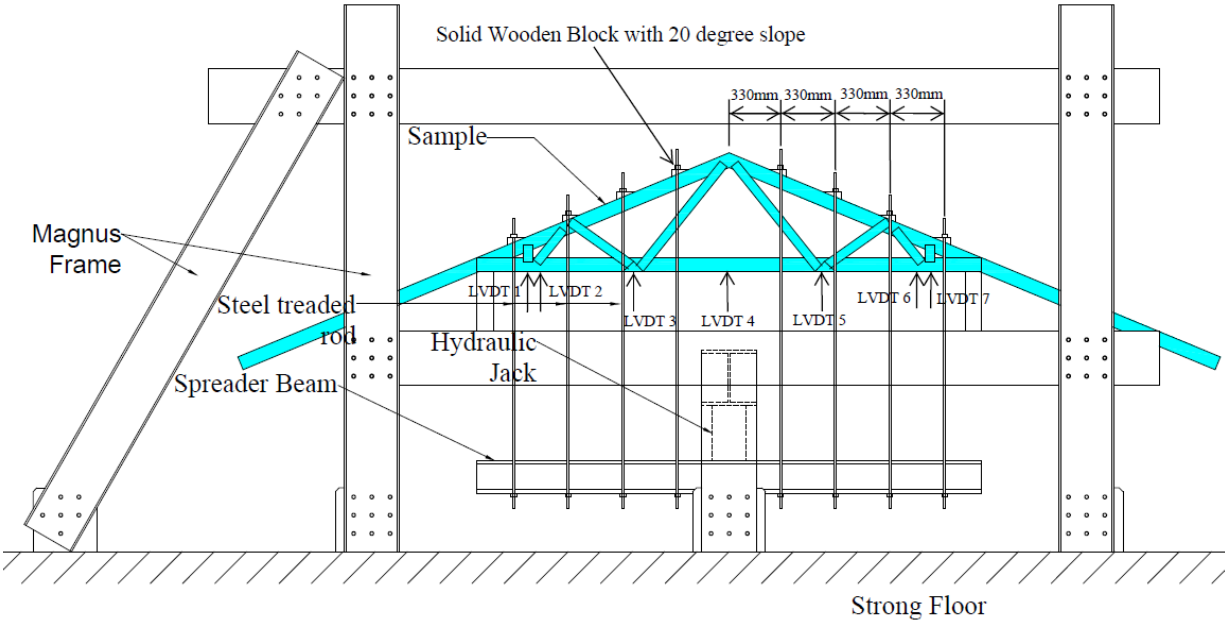


Figure 4: Experimental setting up

## Analytical Investigation

In STAAD Pro analysis, node and line member are used to model the roof truss for analysis. The nodes were created then joined up with line members. Pin and roller supports were used in the modeling roof truss. There were different roof truss models been modeled in this software based on different assumptions. From Figure 5, it can show that the intersection point of the intermediate members located outside the truss structure as those members were not fabricated to connect at the same node on the roof truss. It was hardly to be modeled in STAAD Pro due to the connecting nodes. To get the most similar model to the actual fabricated roof truss, there were four models been modeled.

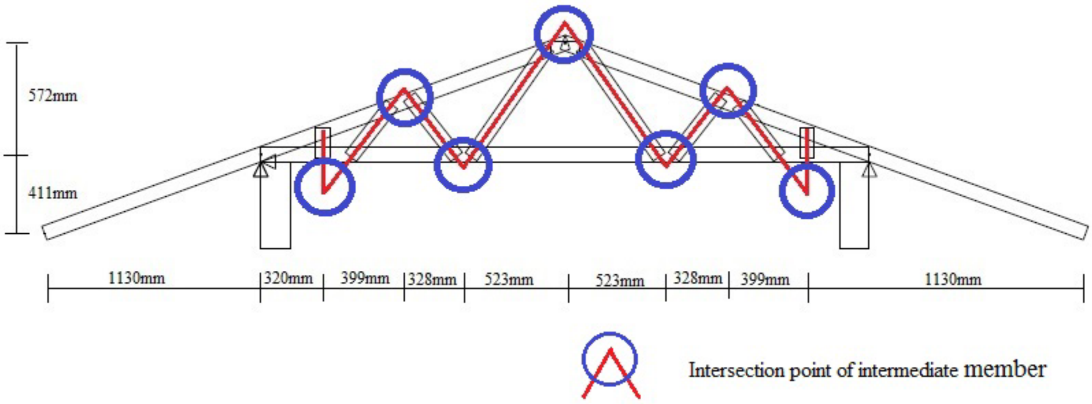


Figure 5: Intersection points of the intermediate members

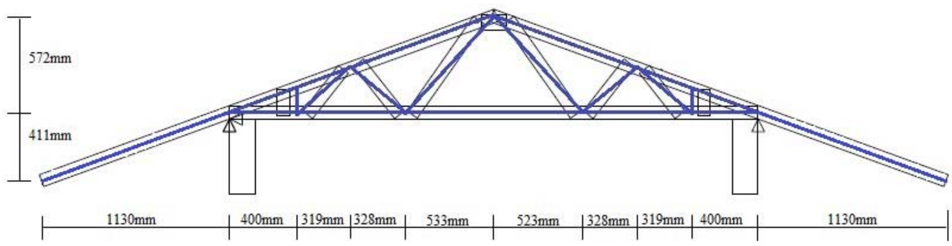


(a) Roof truss-Model 1

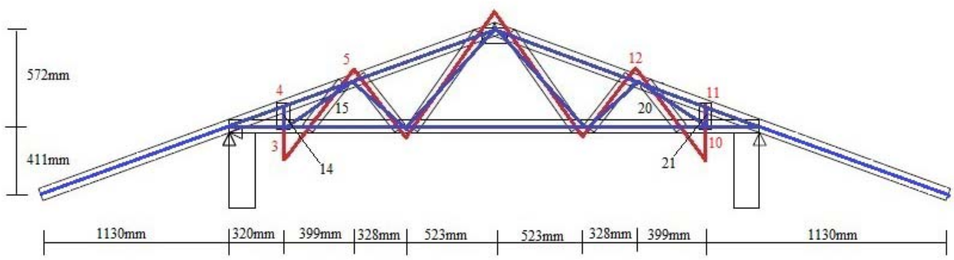


(b) Roof truss-Model 2

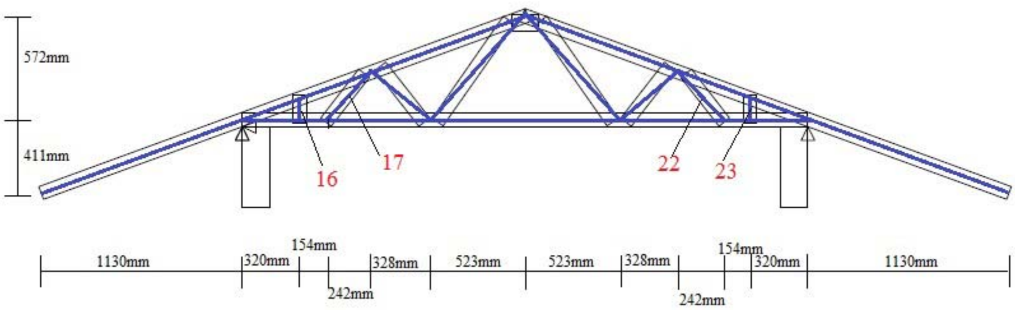


(c) Roof Truss Model 3

Figure 7: STAAD-Pro modeling of roof trusses

In Model 1 (Figure 7a), the joint of intermediate members assumed at the center of two actual intermediate members fabricated on the roof truss. In Figure 7b for Model 2, that was slightly different in terms of the position of Node 3, Node 4, Node10 and Node 11. Member 14 and 21 were modeled same location with the actual roof truss been fabricated. Then the member 15 between Node 3 and Node 5 was had a different slope compared to Model 1 because of the Node 3 was slightly moved towards the support. This situation also applied for the member of member 20. For Model 3 (Figure 7c), the member 16 and 17 were been modeled not to connect in common node. This is same with the member 22 and 23.

Three types of load applied cases were used in every modeling for analysis. This is to analyze the roof truss behaviour more similar to the actual practice by different load acting pattern. In modeling, the loads were applied at the shear center of the members. Below is the load cases used in modeling. For Load Case 1, the maximum loading from experimental results were divided by eight acting points to get the concentrated load applied on top chord. In Load Case 2, maximum load from experiment was divided equally and acted on the five nodes directly. The maximum load from laboratory testing was divided by the total length of top chord and transformed into uniform distributed loading on the top chord. It was assumed that the uniform distributed loading between every two nodes on the top chord will transferred equally to the two nodes nearby.

## Results and Discussions

### *(a) Experimental results*

From the experimental, the deflection of the roof truss was determined due to the load cell applied. The experimental results were shown in the Table 2 and Figure 8. The maximum load can be sustained by the roof truss was 17.4 kN and the maximum deflection is 15.17 mm at LVDT 3.

Table 2: Data from laboratory testing on the roof truss

| LOAD CELL (kN) | LVDT 1 (mm) | LVDT 2 (mm) | LVDT 3 (mm) | LVDT 4 (mm) | LVDT 5 (mm) | LVDT 6 (mm) | LVDT 7 (mm) |
|---|---|---|---|---|---|---|---|
| 17.4 | 8.34 | 12.93 | 15.17 | 14.72 | 14.37 | 12.41 | 7.89 |

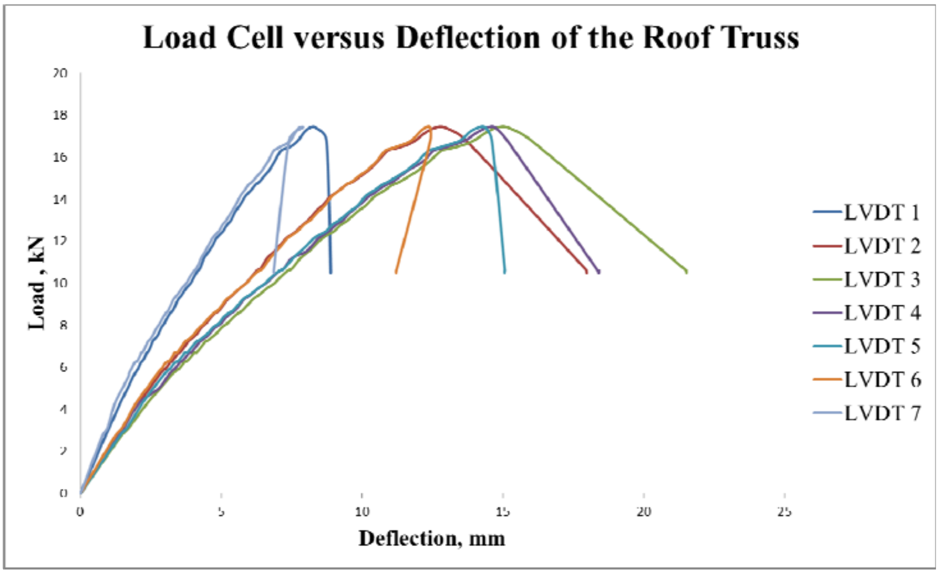


Figure 8: Load-deflection behaviour

Figure 8 presents the relationship between the deflections of the roof truss and load cell applied. Based on this graph, the deflections of the roof truss were increasing with the load applied continuously. When the ultimate load was achieved, the deflections of the roof truss decreased together with the reduction of the applying load. From the graph, it shows that the deflection on left side were higher than right side of the roof truss. This may due to the load applied in laboratory testing was not uniform distributed to the roof truss. As the left side of the roof truss received more loads as compared to the right. Fabrication error may lead the dimensions of the roof truss are not symmetrical and there are some run off on the scale as compared to the roof truss dimension drawing. The dimensions on left side of the roof truss maybe slightly smaller than the right. So, it caused the loads distributed more to the left.

(a) Failure on connection between the intermediate member and top chord

(b) Failure of the roof truss at maximum load applied at front view

(c) Side view of the failure behaviour on roof truss from left hand side

Figure 9: Failure modes

When the load cell reached 17.4 kN as the maximum load applied, the roof truss failed in connection at LVDT 1 which connected the intermediate member to the top chord. According to Figure 9 (a) to (c), the roof truss member performed buckling first following up by the failure of the connection as the screw tore out. The factor lead to buckling happened is the member is under compression. As a result, the compression force causes the buckling happened at the left side of the support as the compression force at support is higher compared to other compression members.

***(b) Analytical results***

From the STAAD Pro analysis, the load case that gave the higher deflection is Load Case 2. It happened in every model analysis results. Below are the maximum deflections of every model analyzed from STAAD Pro.

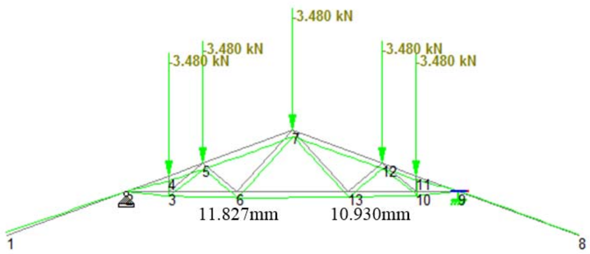


(a) Deflection pattern of Model 1 in Load Case 2

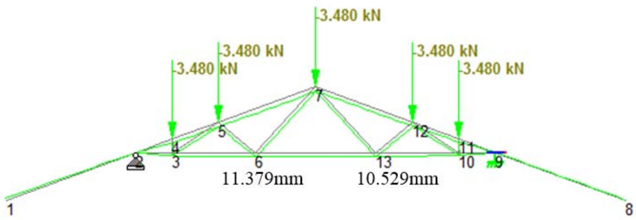


(b) Deflection pattern of Model 2 in Load Case 2

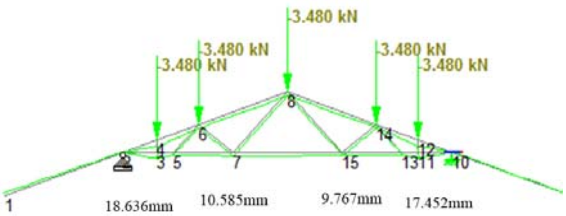


(c) Deflection pattern of Model 3 in Load Case 2

Figure 10: Analytical load-deflection results

As compared the three models, the deflections on left side of roof truss are higher than right side. It may because of the support on left side is pin support and it restraints the x-axis while the support at right side is roller support. With the roller support that release at x-axis, the roof truss tends to move in x-axis when the symmetrical load applied on the top chord of the roof truss. Comparing Model 1 and Model 2, it can conclude that as the intermediate members are located near to support, the deflections will be smaller. In Figure 10, Member 14 in Model 2 is nearer to support as compared to Model 1.

Although Model 1 has the maximum deflection on Node 6, Model 3 has the maximum deflection on Node 3 which is 18.636mm. As the member 16 and 17 were not connected to a same node, it might lead to instability in the structure as Node 3, 5, 6 and 4 created a quadrilateral structure. A quadrilateral structure is less stable than triangular structure. As a result, the Node 3 had maximum deflection. This condition is also happened in Node 11, 13, 14 and 12.

***(c) Comparison between Experimental Results and Analysis Results***

In comparison below, all the models were under critical load case which is Load Case 2.

(i) Experiment Results comparing with Model 1

As mentioned before, the difference between Model 1 and Model 2 is the distance between Member 14 and the support. Member 14 in Model 1 was far to support as compared to Model 2 but they had the close differences deflection value. Model 1 had slightly larger deflection than Model 2 so Model 1 was chosen to compare with experimental results instead of Model 2.

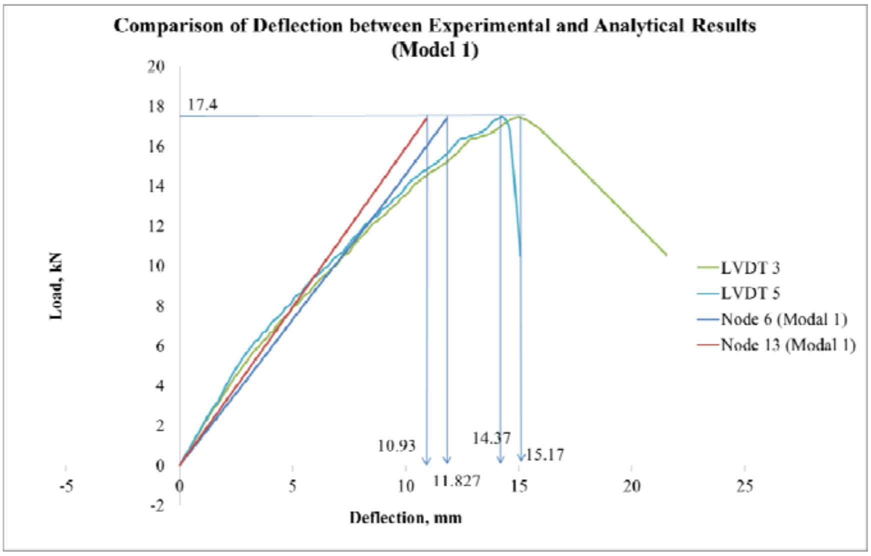


Figure 11: Comparison of Deflection between Experimental and Analytical Results

From Figure 11, it shows the comparison between experimental and analytical results on deflections. At optimum load (17.4kN), the maximum deflection got from laboratory testing was 15.17mm at LVDT 3. It is compared to the STAAD Pro analysis result in Model 1 which had the maximum deflection on Node 6 (11.827mm). It can conclude that the maximum deflection happened on the same location from both experiment and analysis outputs. The different percentage of both data is 15.4 %. There are some reasons that causing the percentage differences among both data. As in laboratory testing, the cold-formed steel is slenderness member and it will experience buckling in compression members which cause to excessive deflection while there was no assuming buckling in software analysis.

(ii) Experimental Results compared with Model 3

As Model 3 was modeled most similar to actual roof truss, its deflection value also been compared to actual roof truss deflection.

In experiment result, the maximum deflection (15.17mm) was at LVDT 3 which near the mid span of the roof truss. While in analytical results of Model 3, the optimum deflection (18.634mm) was at Node 3 near to the support. These results were different with other models in analytical investigation as their maximum deflection near to the mid-span. Although Model 3 was modeled most similar to actual roof truss, the deformations on both investigations were different apart. From Figure 12, it shows the comparison of deflection of both investigations on the node near to support.

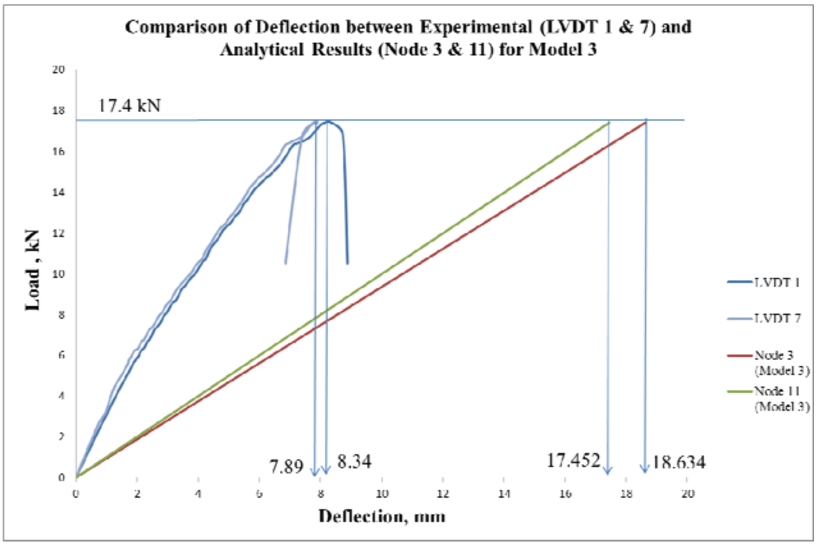


Figure 12: Comparison of deflection between experimental (LVDT 1 & 7) and analytical results (Node 3 & 11) for Model 3

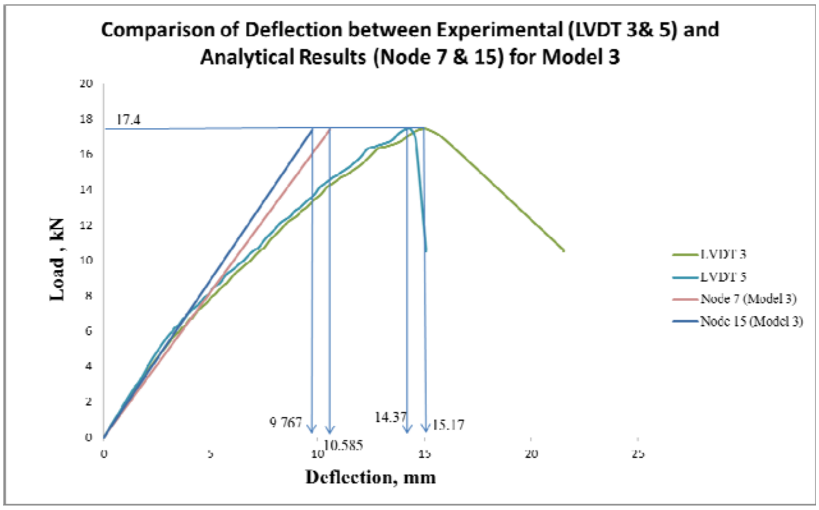


Figure 13: Comparison of deflection between experimental (LVDT 3 & 5) and analytical results (Node 7 & 15) for Model 3

Model 3 had higher deflection. The percentage difference in deflection is 55.24%. In Figure 13, experimental investigation had higher deflection on the node near to the mid-span which was 15.17mm and has 43.32% different in deflection with Model 3. This can be explained as Member 16 is vertical member and was under vertical load at Node 4 in Load Case 2. With the vertical member, the vertical load on Node 4 was directly transferred to Node 3 and made the larger deflection on Node 3. While for actual roof truss, the point load was not applied directly on the vertical member. So, the maximum deflection was near to the mid-span.

## Conclusions

Based on the study carried out, a few outcomes can be made as the conclusions:

(a) From the experiment investigation, the largest deflection happened at LVDT 3 which is 15.17mm at the maximum loads of 17.4kN. The deflection on left side of roof truss is larger than the right due to fabrication error. The failure of the roof truss occurred when buckling happened at the top chord direct to the support on the left and lead to the self-drilling screws wore off.

(b) From analytical results, the top chord of the roof truss was under compression while bottom chord members were under tension. For intermediate members were either experience compressions or tensions. From experimental observation, it is belief that the top chord was under compression which lead to buckling of top chord near the support.

(c) Three models were been analysis with three load cases. Load Case 2 had created critical deflection for all models.

(d) By comparing Model 1 and Model 2, the difference is the distance between Member 14 to the support. From the analytical investigation, the deflection is higher when the distance is far between support and vertical member. So Model 1 has larger deflection as compared to Model 2 as it has longer distance among the two points.

(e) As Model 1 and Model 2 are similar, Model 1 with Load Case 2 was chosen to compare with the experiment results as it has the larger deflection. The percentage differences in deflection between Model 1 and actual roof truss is 15.4 % as it is considered as small differences and valid. The differences between experimental and analytical investigation may cause by different assumptions between both investigations such as the buckling happened in testing while buckling not assumed in modeling.

(f) Although Model 3 was modeled more similar to actual roof truss, it has different deformation behaviour under Load Case 2 compared to laboratory testing results. The highest deflection on actual testing was near to mid-span while the modeling analysis has highest deflection near to support. This is because Load Case 2 in modeling created high deflection as it acting load directly on the vertical member while the load acting on actual roof truss was not direct to the vertical member.

## Acknowledgement

This research is funded by Ministry of Higher Education Malaysia and Universiti Teknologi Malaysia using grants of 4F647, 10H05 and 4F258. The technical supports from Laboratory of Structures and Materials, Faculty of Civil Engineering Universiti Teknologi Malaysia are also appreciated.

## References

[1] South Line Steel Industry. Steel Roof Trusses, Retrieved November 13, 2014, from http://www.southlinesteel.com/

[2] Hibbeler, R. (2010). Engineering mechanics (12th ed.). Singapore: Pearson/Prentice Hall.

[3] Hibbeler, R. (2011). Mechanics of Materials (8th ed.). Singapore: Prentice Hall.

[4] Yu, W., & LaBoube, R. (2010). Cold-formed steel design (4th ed.). Hoboken, N.J.: Wiley.

[5] Hancock, G., Murray, T., & Ellifritt, D. (2001). Cold-formed steel structures to the AISI specification. New York: Marcel Dekker.

[6] Abdel-Rahman, N., & Sivakumaran, K. (1997). Material Properties Models for Analysis of Cold-Formed Steel Members. Journal Of Structural Engineering, 123(9), 1135-1143. doi:10.1061/(asce)0733-9445(1997)123:9(1135)

[7] Dubina, D., Ungureanu, V., & Landolfo, R. (2012). Design of cold-formed steel structures. Berlin: Ernst & Sohn.

[8] Dawe, J., Liu, Y., & Li, J. (2010). Strength and behaviour of cold-formed steel offset trusses. Journal Of Constructional Steel Research, 66(4), 556-565. doi:10.1016/j.jcsr.2009.10.015

[9] Wood, J., & Dawe, J. (2006). Full-Scale Test Behavior of Cold-Formed Steel Roof Trusses. Journal Of Structural Engineering, 132(4), 616-623. doi:10.1061/(asce)0733-9445(2006)132:4(616)